J Math Chem (2015) 53:1393–1411
DOI 10.1007/s10910-015-0495-5

ORIGINAL PAPER

Hopf bifurcation in a fractional diffusion food-limited models with feedback control

Wenzhen Gan[1] · **Canrong Tian**[2] · **Peng Zhu**[1]

Received: 1 February 2015 / Accepted: 18 March 2015 / Published online: 27 March 2015

Abstract In this paper, we consider the direction and stability of Hopf bifurcation induced by time delay in a food-limited models with feedback control and fractional diffusion. By means of analyzing eigenvalue spectrum, we show that the positive equilibrium is locally asymptotically stable in the absence of time delay, but loses its stability via the Hopf bifurcation when the time delay increases beyond a threshold. Using the norm form and the center manifold theory, we investigate the stability and direction of the Hopf bifurcation. The stability of the Hopf bifurcation leads to the emergence of spatial spiral patterns. Numerical calculations are performed to illustrate our theoretical results.

Keywords Fractional diffusion · Time delay · Hopf bifurcation · Spiral pattern

1 Introduction

In this paper, we consider the delayed food-limited model with feedback and fractional diffusion as follows:

The work is partially supported by PRC Grants NSFC 11201406(Tian), 11471145(Zhu), QingLan Project (Zhu) and Research Fund of Jiangsu University of Technology:KYY14010.

✉ Canrong Tian
tiancanrong@163.com

[1] School of Mathematics and Physics, Jiangsu university of Technology, Changzhou 213001, China

[2] Department of Basic Sciences, Yancheng Institute of Technology, Yancheng 224003, China

$$\begin{cases} \frac{\partial u_1}{dt} - D_1 \nabla^\gamma u_1 = u_1 \left[\frac{r(K-u_1)}{K+au_1} - cu_2(x,t-\tau) \right], & (x,t) \in \Omega \times (0,T), \\ \frac{\partial u_2}{dt} - D_2 \nabla^\gamma u_2 = -du_2 + bu_1(x,t-\tau), & (x,t) \in \Omega \times (0,T), \\ \frac{\partial u_1}{\partial \eta} = \frac{\partial u_2}{\partial \eta} = 0, & (x,t) \in \partial\Omega \times (0,T), \\ u_1(x,t) = \psi_1(x,t), u_2(x,t) = \psi_2(x,t), & (x,t) \in \Omega \times [-\tau, 0]. \end{cases} \tag{1.1}$$

Here $u_1 = u_1(x,t)$ denotes the density of a single species and function $u_2 = u_2(x,t)$ is regarded as a "feedback control" variable. r represents the intrinsic growth rate and K represents the carrying capacity. $\frac{r}{a}$ is the replacement of mass in the species at saturation. c is the feedback effort. τ is the time delay, which means that the effect of feedback control is not instantaneous, but mediated by some time lag required for maturity of species. d and b are the coefficients of the feedback function. For more details in the feedback control system, please see [1,2]. K, a, c, d, b, and τ are positive constants. ∇^γ $(1 < \gamma < 2)$ is a fractional power of the Laplacian. D_1 and D_2 are fractional dispersal rates. The fractional Laplacian implies that the species possess the continuous time random walk with a Lévy distribution where jump length has a heavy tailed variance. Ω is a bounded domain in $\mathbf{R}^2$ with boundary $\partial\Omega$ and η denotes the outward normal derivative on $\partial\Omega$. The initial values $\psi_1(x,t)$ and $\psi_2(x,t)$ are non-negative smooth functions which are not identically zero. The homogeneous Neumann boundary conditions indicate that there is no species flux across the boundaries.

The motivation and derivation of the fractional operator in Eq. (1.1) are as follows. We take $u(x,t)$ as an example in an isotropic setting [3]. The Fick's Law states that mass is transported at a flux $V = -D\nabla u$ through a unit area. Taking into account the mass conservation, i.e.,

$$\frac{\partial u}{\partial t} = -\nabla \cdot V, \tag{1.2}$$

we have the classic diffusion equation

$$\frac{\partial u}{\partial t} = \nabla \cdot (D \nabla u). \tag{1.3}$$

The fundamental assumption behind this approach is homogeneous media, which is questioned for heterogeneous media [4], because in heterogeneous structures such as those processing spatial connectivity, movement of particles may be facilitated with a certain scale–so-called superdiffusion. Since the spatial complexity of the environment can impose geometric constraints on the transport processes on all length scales, resulting in temporal correlations on all time scales, inhomogeneous media can therefore alter the laws of Markow diffusion, leading to long range fluxes and non-Gaussian heavy tailed profiles [5,6] and thus these motions may no longer follow Fick's Law [7]. This is also related to homogenisation principle which is fundamental for predicting macroscopic properties from microscopic features [8]. The macroscopic and microscopic is often assumed to be independent, but in some settings the independency breaks down and the homogenisation principle does not hold. It is in this context that fractional models can offer insights that traditional approaches do not offer, especially for the case of diffusion in heterogeneous environments.

A diffusion equation with fractional operator can be derived by replacing Fick's Law for the flux V by its fractional counterpart [9],

$$V = -D\nabla^{\beta} u, \tag{1.4}$$

where $\beta = \gamma - 1$. The fractional operator $\nabla^{\beta} = \left(\frac{\partial^{\beta}}{\partial x^{\beta}}, \frac{\partial^{\beta}}{\partial y^{\beta}}\right)$ is the Weyl fractional gradient in two dimensional space, and

$$\frac{\partial^{\beta}}{\partial x^{\beta}} u(x, y) = -\frac{\sec(\pi\gamma/2)}{2\Gamma(1-\beta)} \frac{\partial}{\partial x} \int_{-\infty}^{\infty} \frac{u(s, y)}{|x - s|^{\beta}} ds, \tag{1.5}$$

with similar expressions for $\frac{\partial^{\beta}}{\partial y^{\beta}}$ [10]. The fractional Fick's Law (1.4), which implies spatial and temporal non locality, can be rigorously derived be means of spatial averaging theorems and measurable functions [11]. Combining the fractional Fick's Law and the mass conservation (1.2) leads to

$$\frac{\partial u}{\partial t} = -\nabla \cdot (-D\nabla^{\beta} u), \tag{1.6}$$

which can be equivalently rewritten as

$$\frac{\partial u}{\partial t} = D\nabla^{\gamma} u. \tag{1.7}$$

It is verified that the Fourier transform of $\nabla^{\gamma} u$ satisfies $\mathcal{F}(\nabla^{\gamma} u) = -|k|^{\gamma} \mathcal{F}(u)$, where k is the wavenumber. In higher dimension, the Laplacian is replaced by the operator $\nabla^{\gamma} = -(-\Delta)^{\gamma/2}$.

Pattern formation in reaction-diffusion systems with anomalous diffusion has received considerable attention [12–17]. For instance, it was shown that the Lévy flights type superdiffusion induces the formation of Turing pattern [15]. It was also shown that subdiffusion suppresses the formation of Turing pattern [14]. In [16,17], Turing patterns were induced by the anomalous diffusion both in Brusselator chemical system and Boissonade chemical system. Additionally, in systems with Lévy flights, the emergence of spiral waves and chemical turbulence from the nonlinear dynamics of oscillating reaction-diffusion patterns was investigated in [18]. A natural question is how fractional diffusion affects the spiral waves from the mathematical viewpoint. Our aim is to show that the Hopf bifurcation causes the reaction-diffusion system with fractional diffusion to generate the spiral patterns.

The remaining parts of the paper are constructed in the following way. In Sect. 2, we get the local asymptotic stability and Hopf bifurcation of the positive equilibrium of system (1.1). The direction and stability of Hopf bifurcation are discussed by taking time delay as a bifurcation parameter in Sect. 3. In Sect. 4 we perform some numerical simulation to illustrate our theoretical analysis. The paper ends with a brief discussion.

2 Stability of positive equilibrium and the existence of Hopf bifurcation

In this section, we investigate the local asymptotic stability of the positive equilibrium and the existence of Hopf bifurcation.

It is easy to veify that the system (1.1) has an unique positive equilibrium $\mathbf{u}^* = (u_1^*, u_2^*)$, where $u_1^* = \frac{-(bcK+dr)+\sqrt{(bcK+dr)^2+4abcdrK}}{2abc}$, $u_2^* = \frac{bu_1^*}{d}$. Linearing the system (1.1) around $\mathbf{u}^*$ gives

$$\begin{cases} \frac{\partial u_1}{\partial t} - D_1\nabla^\gamma u_1 = u_1\left[-\frac{rK(1+a)u_1^*}{(K+au_1^*)^2}u_1 - cu_1^*u_2(x,t-\tau)\right], & (x,t)\in\Omega\times(0,T),\\ \frac{\partial u_2}{\partial t} - D_2\nabla^\gamma u_2 = bu_1(x,t-\tau) - du_2, & (x,t)\in\Omega\times(0,T),\\ \frac{\partial u_1}{\partial \eta} = \frac{\partial u_2}{\partial \eta} = 0, & (x,t)\in\partial\Omega\times(0,T),\\ u_1(x,t) = \varphi_1(x,t) - u_1^*, u_2(x,t) = \varphi_2(x,t) - u_2^*, & (x,t)\in\Omega\times(-\infty,0]. \end{cases} \tag{2.1}$$

Since the boundary condition is homogeneous Neumann on the domain Ω, the appropriate eigenfunction of Eq. (2.1) is

$$(u_1, u_2) = (c_1, c_2)e^{\lambda t}coskx, \tag{2.2}$$

where λ is the eigenvalue and k is the wavenumber. Consequently, substituting (2.2) into Eq. (2.1) yields

$$\begin{cases} (\lambda c_1 + D_1k^\gamma c_1)e^{\lambda t}\cos kx = \left[-\frac{rK(1+a)u_1^*}{(K+au_1^*)^2}c_1 - cu_1^*e^{-\lambda\tau}c_2\right]e^{\lambda t}\cos kx,\\ (\lambda c_2 + D_2k^\gamma c_2)e^{\lambda t}\cos kx = (be^{-\lambda\tau}c_1 - dc_2)e^{\lambda t}\cos kx. \end{cases} \tag{2.3}$$

Therefore, we can get that nontrivial solution to Eq. (2.3) exists if and only if

$$\det\begin{pmatrix} \lambda + D_1k^\gamma + \frac{rK(1+a)u_1^*}{(K+au_1^*)^2} & cu_1^*e^{-\lambda\tau}\\ -be^{-\lambda\tau} & \lambda + D_2k^\gamma + d \end{pmatrix} = 0. \tag{2.4}$$

By simple calculation, we obtain the following characteristic equation:

$$\nabla^\gamma(\lambda,\tau) = \lambda^2 + A_k\lambda + B_k + C_ke^{-2\lambda\tau} = 0, \tag{2.5}$$

where

$$\begin{aligned} &A_k = D_1k^\gamma + D_2k^\gamma + \frac{rK(1+a)u_1^*}{(K+au_1^*)^2} + d,\ B_k = \left(D_1k^\gamma + \frac{rK(1+a)u_1^*}{(K+au_1^*)^2}\right)(D_2k^\gamma + d)\\ &C_k = bcu_1^*. \end{aligned} \tag{2.6}$$

We now investigate the local asymptotic stability of $\mathbf{u}^*$ for system (1.1). It is well known that $\mathbf{u}^*$ is locally asymptotically stable if all roots λ of the characteristic Eq. (2.5) satisfy $Re\{\lambda\} < 0$.

Theorem 2.1 *Assume that the parameters of system (1.1) satisfy*

$$(G_1): \frac{drK(1+a)}{(K+au_1^*)^2} < bc,$$

then

(i) If the delay is absent, that is $\tau = 0$, then $\mathbf{u}^*$ of system (1.1) is locally asymptotically stable.

(ii) If the delay is present, that is $\tau \neq 0$, then there exists a critical point τ^*. $\mathbf{u}^*$ is locally asymptotically stable when $\tau < \tau^*$ and $\mathbf{u}^*$ is locally asymptotically unstable when $\tau \geq \tau^*$.

Proof We first prove part (i). Eq. (2.5) becomes

$$\lambda^2 + A_k\lambda + B_k + C_k = 0 \tag{2.7}$$

when $\tau = 0$. It follows from the assumption (G_1) that $A_k > 0$ and $B_k + C_k > 0$. Then the real parts of the roots of Eq. (2.7) are negative. Thus, by virture of the Routh–Hurwitz theorem, $\mathbf{u}^*$ is asymptotic stable when $\tau = 0$. This completes the proof of part (i).

Next, we prove part (ii). Suppose that $\lambda = i\omega$, with $w > 0$, is a root of Eq. (2.5), then we obtain

$$(i\omega)^2 + i\omega A_k + B_k + C_k e^{-2i\omega\tau} = 0.$$

Separating the real parts and imaginary parts, we have

$$\begin{cases} \omega^2 - B_k = C_k \cos 2\omega\tau, \\ A_k\omega = C_k \sin 2\omega\tau, \end{cases} \tag{2.8}$$

which leads to

$$\omega^4 + (A_k^2 - 2B_k)\omega^2 + B_k^2 - C_k^2 = 0, \tag{2.9}$$

where

$$\begin{aligned} A_k^2 - 2B_k &= \left(D_1k^\gamma + \frac{rK(1+a)u_1^*}{(K+au_1^*)^2}\right)^2 + (D_2k^\gamma + d)^2 > 0, \\ B_k^2 - C_k^2 &= \left[\left(D_1k^\gamma + \frac{rK(1+a)u_1^*}{(K+au_1^*)^2}\right)(D_2k^\gamma + d) - bcu_1^*\right] \\ &\quad \times \left[\left(D_1k^\gamma + \frac{rK(1+a)u_1^*}{(K+au_1^*)^2}\right)(D_2k^\gamma + d) + bcu_1^*\right]. \end{aligned} \tag{2.10}$$

For some fixed k, it is easy to check that $B_k^2 - C_k^2 < 0$ when (G_1) is satisfied. Therefore, Eq. (2.9) has a unique positive real root,

$$\omega_k = \sqrt{\frac{-(A_k^2-2B_k)+\sqrt{(A_k^2-2B_k)^2-4(B_k^2-C_k^2)}}{2}}. \tag{2.11}$$

Then Eq. (2.5) has pure imaginary roots $\pm i\omega^*$ when

$$\tau_k^j = \frac{1}{2\omega_k}\arctan\frac{A_k\omega_k}{\omega_k^2 - B_k} + \frac{2j\pi}{\omega_k},\ j = 0, 1, 2, \cdots. \tag{2.12}$$

Set $\tau^* = \tau_k^0$ and $\omega^* = \omega_k$. Then, by the Butler's Lemma [19] proven in Appendix A, $\mathbf{u}^*$ is unstable for $\tau > \tau^*$. On the other hand, if $\tau \in [0, \tau^*)$, then Eq. (2.5) has no roots on the imaginary axis. Making use of the eigenvalue theory of [20], the sum of orders of the zeros of Eq. (2.5) for $\tau \in [0, \tau^*)$ is equal to Eq. (2.7). Then Eq. (2.5) for $\tau \in [0, \tau^*)$ only has negative real part roots, which implies that $\mathbf{u}^*$ is locally asymptotically stable for $\tau < \tau^*$.This completes the proof of part (ii). □

Theorem 2.2 *Under the assumption (G_1), solutions of the system (1.1) undergo a Hopf bifurcation at $\mathbf{u}^*$ when $\tau = \tau^*$.*

Proof Denote $\lambda(\tau) = \sigma(\tau) + i\omega(\tau)$, is the root of Eq. (2.5) satisfying $\sigma(\tau^*) = 0$ and $\omega(\tau^*) = \omega^*$. Substituting $\lambda(\tau)$ into Eq. (2.5) and taking the derivative of λ with respect to τ, we obtain

$$\left[\frac{d\lambda}{d\tau}\right]^{-1} = \frac{(2\lambda + A_k)e^{2\lambda\tau}}{2\lambda C_k} - \frac{\tau}{\lambda}.$$

Note that

$$\begin{aligned} sign\left\{\frac{dRe(\lambda(\tau))}{d\tau}\right\}_{\tau=\tau^*} &= sign\left\{Re\left[\frac{d\lambda(\tau)}{d\tau}\right]\right\}_{\tau=\tau^*} \\ &= sign\left\{Re\left[\frac{d\lambda(\tau)}{d\tau}\right]^{-1}\right\}\tau = \tau^* \end{aligned}$$

which, together with (2.8), (2.11) and (2.12), leads to

$$\begin{aligned} &sign\left\{Re\left[\frac{d\lambda(\tau)}{d\tau}\right]^{-1}\right\}_{\tau=\tau^*} \\ &= sign\left\{Re\left[\frac{d\lambda(\tau)}{d\tau}\right]^{-1}\right\}_{\lambda=i\omega^*} \\ &= sign\left\{Re\left[\frac{(2i\omega^* + A_k)(cos2\tau^*\omega^* + isin2\tau^*\omega^*)}{2i\omega^* C_k} - \frac{\tau^*}{i\omega^*}\right]\right\} \\ &= sign\left\{\frac{2\omega^{*3} + (A_k^2 - 2B_k)\omega^*}{2\omega^* C_k^2}\right\}. \end{aligned}$$

From (2.10), we find that the transversality condition

$$sign\left\{\frac{dRe[\lambda(\tau)]}{d\tau}\right\}_{\tau=\tau^*} > 0 \tag{2.13}$$

holds. Therefore, solutions of the system (1.1) undergo a Hopf bifurcation at $\mathbf{u}^*$ when $\tau = \tau^*$. □

3 The direction and stability of the Hopf bifurcation

In the previous section, we obtained condition (G_1) ensuring system (1.1) undergoes a Hopf bifurcation at $\mathbf{u}^*$. In this section, we shall establish the explicit formula for determining the direction and stability of periodic solutions bifurcating from $\mathbf{u}^*$ at τ^*, by using normal form theory and center manifold argument presented in Hassard et al. [21] .

By the change of variables $u_1(x,t) - u_1^* \mapsto w_1(x,t)$, $u_2(x,t) - u_2^* \mapsto w_2(x,t)$ and $\tau - \tau^* \mapsto \mu$ and by rescaling the time $t \mapsto (t/\tau^*)$, the system (1.1) can be written as

$$\begin{cases} \partial_t w_1 = (\tau^*+\mu)\Big[D_1\nabla^\gamma w_1 - \frac{drK(1+a)u_1^*}{(K+au_1^*)^2}w_1 - cu_1^* w_1(x,t-1) - cw_1 w_2(x,t-1) \\ \qquad\qquad - \frac{rK^2(1+a)}{K+au_1^*)^3}w_1^2 + \frac{rK^2a(1+a)}{(K+au_1^*)^4}w_1^3 + \Sigma_{i>3}\frac{(-1)^{i-1}rK^2a^{i-2}(1+a)}{(K+au_1^*)^{i+1}}w_1^i\Big], \\ \partial_t w_2 = (\tau^*+\mu)[D_2\nabla^\gamma w_2 - dw_2 + bw_1(x,t-1)]. \end{cases} \tag{3.1}$$

Throughout this section, we refer to Hassard et al. [21] for explanations of notations involved. Then the system (3.1) is transformed into a functional differential equation in $\mathbf{C} := C([0,1], R^2)$.

$$\dot{\mathbf{w}}(t) = L_\mu(\mathbf{w}_t) + f(\gamma, \mathbf{w}_t), \tag{3.2}$$

where $\mathbf{w}(x,t) = (w_1(x,t), w_2(x,t))^T \in \mathbb{R}^2$ and $L_\mu : \mathbf{C} \to \mathbb{R}^2$, $f : \mathbb{R}\times\mathbf{C} \to \mathbb{R}^2$ are respectively represented by

$$\begin{aligned} L_\mu(\phi) = (\tau^*+\mu)&\begin{pmatrix} D_1\nabla^\gamma - \frac{rK(1+a)u_1^*}{(K+au_1^*)^2} & 0 \\ 0 & D_2\nabla^\gamma - d \end{pmatrix}\begin{pmatrix}\phi_1(0)\\ \phi_2(0)\end{pmatrix} \\ &+ (\tau^*+\mu)\begin{pmatrix} 0 & -cu_1^* \\ b & 0 \end{pmatrix}\begin{pmatrix}\phi_1(-1)\\ \phi_2(-1)\end{pmatrix}, \end{aligned} \tag{3.3}$$

and

$$f(\gamma,\phi) = (\tau^*+\mu)\begin{pmatrix} -c\phi_1(0)\phi_2(-1) - \frac{rK^2(1+a)}{(K+au_1^*)^3}\phi_1^2(0) + \frac{rK^2a(1+a)}{(K+au_1^*)^4}\phi_1^3 + D \\ 0 \end{pmatrix} \tag{3.4}$$

where $D = \Sigma_{i>3} \frac{(-1)^{i-1} r K^2 a^{i-2}(1+a)}{(K+au_1^*)^{i+1}} \phi_1^i(0)$, $\phi(\theta) = (\phi_1(\theta), \phi_2(\theta)) \in \mathbf{C}$. Since $\pm i\omega^*$ are a pair of simple purely imaginary eigenvalues of the liner operator L_μ, L_μ is transformed to

$$L_\mu(\phi) = (\tau^* + \mu)\begin{pmatrix} -D_1 k^\gamma - \frac{rK(1+a)u_1^*}{(K+au_1^*)^2} & 0 \\ 0 & -D_2 k^\gamma - d \end{pmatrix}\begin{pmatrix} \phi_1(0) \\ \phi_2(0) \end{pmatrix} + (\tau^* + \mu)\begin{pmatrix} 0 & -cu_1^* \\ b & 0 \end{pmatrix}\begin{pmatrix} \phi_1(-1) \\ \phi_2(-1) \end{pmatrix}. \tag{3.5}$$

By the Riesz representation theorem, there exists a 2×2 matrix $\eta(\theta, \mu)$, $\theta \in [-1, 0]$, whose elements are functions of bounded variation such that

$$L_\mu \phi = \int_{-1}^{0} [d\eta(\theta, \mu)]\phi(\theta), \text{ for } \phi \in \mathbf{C}. \tag{3.6}$$

In fact, we can choose

$$\eta(\theta, \mu) = (\tau^* + \mu)\begin{pmatrix} -D_1 k^\gamma - \frac{rK(1+a)u_1^*}{(K+au_1^*)^2} & 0 \\ 0 & -D_2 k^\gamma - d \end{pmatrix}\delta(\theta) + (\tau^* + \mu)\begin{pmatrix} 0 & -cu_1^* \\ b & 0 \end{pmatrix}\delta(\theta + 1), \tag{3.7}$$

where δ is a Dirac delta function. Then (3.6) is satisfied. For $\phi \in \mathbf{C}^1([-1, 0], \mathbb{R}^2)$, define

$$A(\mu)\phi = \begin{cases} \frac{d\phi(\theta)}{d\theta}, & \text{for} \quad \theta \in [-1, 0), \\ \int_{-1}^{0} [d\eta(s, \mu)]\phi(s), & \text{for} \quad \theta = 0, \end{cases} \tag{3.8}$$

and

$$R(\mu)\phi = \begin{cases} 0, & \text{for} \quad \theta \in [-1, 0), \\ f(\mu, \phi), & \text{for} \quad \theta = 0. \end{cases} \tag{3.9}$$

Then the system (3.2) is equivalent to the following operator equation

$$\dot{\mathbf{w}}_t = A(\mu)(\mathbf{w}_t) + R(\mu)(\mathbf{w}_t). \tag{3.10}$$

As in [21], $\mathbf{w}_t(\theta) = \mathbf{w}(t + \theta)$ for $\theta \in [-1, 0]$. Now, for $\psi \in C^1([0, 1], (\mathbb{R}^2)^*)$, we define

$$A^*\psi(s) = \begin{cases} -\frac{d\psi(s)}{ds}, & \text{for} \quad s \in [-1, 0), \\ \int_{-1}^{0} \psi(-t) d\eta^T(t, 0), & \text{for} \quad s = 0, \end{cases} \tag{3.11}$$

and a bilinear inner product $< \cdot, \cdot >$ by

$$\langle \psi(s), \phi(\theta) \rangle = \bar{\psi}(0)\phi(0) - \int_{-1}^{0} \int_{0}^{\theta} \bar{\psi}(\xi - \theta) d\eta(\theta) \phi(\xi) d\xi, \tag{3.12}$$

where $\eta(\theta) = \eta(\theta, 0)$. Then $A(0)$ and A^* are adjoint operators.

From the discussion in Theorem 2.1, we know that $\pm i\omega^*\tau^*$ are eigenvalues of $A(0)$. Thus they are also eigenvalues of A^*. Next, we calculate the eigenvector $q(\theta)$ of $A(0)$ belonging to the eigenvalue $i\omega^*\tau^*$ and the eigenvector $q^*(s)$ of A^* belonging to the eigenvalue $-i\omega^*\tau^*$. Let $q(\theta) = (q_1, q_2)^T e^{i\omega^*\tau^*\theta}$, $-1 < \theta \leq 0$. From the above discussion, we know that $A(0)q(\theta) = i\omega^*\tau^* q(\theta)$, i.e.,

$$\begin{pmatrix} -D_1 k^\gamma - \frac{rK(1+a)u_1^*}{(K+au_1^*)^2} - i\omega^* & -cu_1^* e^{-i\omega^*\tau^*} \\ be^{-i\omega^*\tau^*} & -D_2 k^\gamma - d - i\omega^* \end{pmatrix} \begin{pmatrix} q_1 \\ q_2 \end{pmatrix} = 0.$$

Therefore, we have

$$q(\theta) = \left(1, \frac{be^{-i\omega^*\tau^*}}{D_2 k^\gamma + d + i\omega^*}\right)^T e^{i\omega * \tau^* \theta}. \tag{3.13}$$

Similarly, let $q^*(s) = M(q_1^*, q_2^*)e^{i\omega^*\tau^* s}$ be the eigenvector of A^* corresponding to $-i\omega^*\tau^*$. Then we have the following relationship: $A^* q^*(s) = -i\omega^*\tau^* q^*(s)$, i.e.,

$$\begin{pmatrix} -D_1 k^\gamma - \frac{rK(1+a)u_1^*}{(K+au_1^*)^2} + i\omega^* & be^{i\omega^*\tau} \\ -cu_1^* e^{i\omega^*\tau} & -D_2 k^\gamma - d + i\omega^* \end{pmatrix} \begin{pmatrix} q_1^* \\ q_2^* \end{pmatrix} = 0.$$

Hence, we have

$$q^*(s) = M\left(\frac{D_2 k^\gamma + d - i\omega^*}{-cu_1^* e^{i\omega^*\tau}}, 1\right) e^{i\omega^*\tau^* s}. \tag{3.14}$$

In order to ensure $\langle q^*(s), q(\theta) \rangle = 1$, we need to determine the value of M. By (3.12), we have

$$\begin{aligned} \langle q^*(s), q(\theta) \rangle &= \bar{q}^*(0)q(0) - \int_{-1}^{0} \int_{0}^{\theta} \bar{q}^*(\xi - \theta) d\eta(\theta) q(\xi) d\xi \\ &= \bar{M}(\bar{q}_1^*, \bar{q}_2^*)(q_1, q_2)^T \\ &\quad - \int_{-1}^{0} \int_{0}^{\theta} \bar{M}(\bar{q}_1^*, \bar{q}_2^*) e^{-i\omega^*\tau^*(\xi-\theta)} d\eta(\theta)(q_1, q_2)^T e^{i\omega^*\tau^*\xi} d\xi \\ &= \bar{M}\bar{q}_1^* \left(q_1 + \tau^* e^{-i\omega^*\tau^*}(0q_1 - cu_1^* q_2)\right) \end{aligned}$$

$$+\bar{M}\bar{q}_2^*\left(q_2+\tau^* e^{-i\omega^*\tau^*}(bq_1-0q_2)\right)$$
$$=\bar{M}\left(\bar{q}_1^* q_1+\bar{q}_2^* q_2-cu_1^* q_2\tau^* e^{-i\omega^*\tau^*}+b\tau^* q_1 e^{-i\omega^*\tau^*}\right).$$

Since $q_1=1,\ q_2^*=1$, we can choose M as

$$\bar{M}=1/\left(\bar{q}_1^*+q_2-cu_1^* q_2\tau^* e^{-i\omega^*\tau^*}+b\tau^* e^{-i\omega^*\tau^*}\right), \tag{3.15}$$

where $\bar{M}$ is the conjugate imaginary of M.

Next, we compute the coordinate to describe the center manifold C_0 at $\mu=0$. Let w_t be the solution of (3.10) when $\mu=0$. Define

$$\begin{aligned} z(t)&=\langle q^*, w_t\rangle,\\ W(t,\theta)&=w_t(\theta)-2Re\{z(t)q(\theta)\}. \end{aligned} \tag{3.16}$$

On the center manifold C_0, we have $W(t,\theta)=W(z(t),\bar{z}(t),\theta)$, where

$$W(z(t),\bar{z}(t),\theta)=W_{20}(\theta)\frac{z^2}{2}+W_{11}(\theta)z\bar{z}+W_{02}(\theta)\frac{\bar{z}^2}{2}+\cdots. \tag{3.17}$$

In fact, z and $\bar{z}$ are local coordinates for the center manifold C_0 in the direction of q^* and $\bar{q^*}$ respectively. Note that W is real if w_t is real. We consider only real solutions. For solution $w_t\in C_0$ of (3.10), since $\gamma=0$ and (3.16), we have

$$\begin{aligned} \dot{z}(t)&=\langle q^*, \dot{w}_t\rangle\\ &=i\omega^*\tau^* z+\bar{q^*}(0)f(0,W(z,\bar{z},0)+2Re\{zq(0)\})\\ &\triangleq i\omega^*\tau^* z+\bar{q^*}(0)f_0(z,\bar{z}). \end{aligned} \tag{3.18}$$

We rewrite above equation as

$$\dot{z}(t)=i\omega^*\tau^* z+g(z,\bar{z}), \tag{3.19}$$

where

$$\begin{aligned} g(z,\bar{z})&=\bar{q^*}(0)f_0(z,\bar{z})\\ &=g_{20}\frac{z^2}{2}+g_{11}z\bar{z}+g_{02}\frac{\bar{z}^2}{2}+g_{21}\frac{\bar{z}^2 z}{2}+\cdots. \end{aligned} \tag{3.20}$$

In the following, our motivation is to expand g in powers of z and $\bar{z}$ and then obtain the coefficients. Combing (3.16) with (3.17), we obtain that

$$\begin{aligned} w_t(\theta)&=W(t,\theta)+2Re\{z(t)q(\theta)\}\\ &=W_{20}(\theta)\frac{z^2}{2}+W_{11}(\theta)z\bar{z}+W_{02}(\theta)\frac{\bar{z}^2}{2}+zq+\bar{z}\bar{q}+\cdots \end{aligned}$$

$$= W_{20}(\theta)\frac{z^2}{2} + W_{11}(\theta)z\bar{z} + W_{02}(\theta)\frac{\bar{z}^2}{2} + (q_1, q_2)^T e^{i\omega^*\tau^*\theta} z$$
$$+ (\bar{q}_1, \bar{q}_2)^T e^{-i\omega^*\tau^*\theta}\bar{z} + \cdots \tag{3.21}$$

Substituting (3.4) and (3.21) into (3.20), we have

$$\begin{aligned} g(z,\bar{z}) &= \bar{q^*}(0) f_0(z,\bar{z}) = \bar{q^*}(0) f_0(z, w_t) \\ &= \bar{M}\tau^*(\bar{q}_1^*, 1)\begin{pmatrix} -c\phi_1(0)\phi_2(-1) - \frac{rK^2(1+a)}{(K+au_1^*)^3}\phi_1^2(0) + \frac{rK^2a(1+a)}{(K+au_1^*)^4}\phi_1^3 + D \\ 0 \end{pmatrix} \\ &= p_1 z^2 + p_2 z\bar{z} + p_3\bar{z}^2 + p_4 z^2\bar{z} + h.o.t., \end{aligned} \tag{3.22}$$

where $h.o.t.$ stands for higher order terms, $W_{mn}(\theta) = (W_{mn}^{(1)}(\theta), W_{mn}^{(2)}(\theta))^T$ and

$$\begin{aligned} p_1 &= \bar{M}\tau^*\bar{q}_1^*\left[-cq_2 e^{-i\omega^*\tau^*} - \frac{rK^2(1+a)}{(K+au_1^*)^3}\right], \\ p_2 &= 2\bar{M}\tau^*\bar{q}_1^*\left[-\frac{rK^2(1+a)}{(K+au_1^*)^3} - cRe\left\{\bar{q}_2 e^{i\omega^*\tau^*}\right\}\right], \\ p_3 &= \bar{M}\tau^*\bar{q}_1^*\left[-c\bar{q}_2 e^{i\omega^*\tau^*} - \frac{rK^2(1+a)}{(K+au_1^*)^3}\right], \\ p_4 &= \bar{M}\tau^*\bar{q}_1^*\left[\left(\frac{-rK^2(1+a)}{(K+au_1^*)^3} - \frac{1}{2}c\bar{q}_2 e^{i\omega^*\tau^*}\right)W_{20}^{(1)}(0)\right. \\ &\quad + \left(-\frac{2rK^2(1+a)}{(K+au_1^*)^3} - cq_2 e^{-i\omega^*\tau^*}\right)W_{11}^{(1)}(0) \\ &\quad \left. -\frac{1}{2}cW_{20}^{(2)}(-1) - cW_{11}^{(2)}(-1) + \frac{3rK^2a(1+a)}{(K+au_1^*)^4}\right] \end{aligned} \tag{3.23}$$

Comparing the coefficients in (3.20) and (3.22), we have

$$g_{20} = 2p_1,\ g_{11} = p_2,\ g_{02} = 2p_3,\ g_{21} = 2p_4. \tag{3.24}$$

Since g_{21} depends on $W_{20}(\theta)$ and $W_{11}(\theta)$, we need to find the values of $W_{20}(\theta)$ and $W_{11}(\theta)$. From (3.2) and (3.16), we have

$$\begin{aligned} \dot{w} &= \dot{w}_t - \dot{z}q - \dot{\bar{z}}\bar{q} \\ &= \begin{cases} AW - 2Re\{\bar{q}^*(0) f_0 q(\theta)\}, & -1 \le \theta < 0, \\ AW - 2Re\{\bar{q}^*(0) f_0 q(\theta)\} + f_0, & \theta = 0, \end{cases} \\ &\triangleq AW + H(z,\bar{z},\theta), \end{aligned} \tag{3.25}$$

where

$$H(z,\bar{z},\theta) = H_{20}\frac{z^2}{2} + H_{11}z\bar{z} + H_{02}\frac{\bar{z}^2}{2} + \cdots . \tag{3.26}$$

From (3.17), we have

$$\begin{aligned}\dot{w} &= \dot{w}_z\dot{z}(t) + \dot{w}_{\bar{z}}\dot{\bar{z}}(t)\\ &= (W_{20}(\theta)z + W_{11}(\theta)\bar{z} + \cdots)(i\omega^*\tau^*z(t) + g(z,\bar{z}))\\ &\quad + (W_{11}(\theta)z + W_{02}(\theta)\bar{z} + \cdots)(-i\omega^*\tau^*\bar{z}(t) + \bar{g}(z,\bar{z})).\end{aligned} \tag{3.27}$$

It follows from (3.20) that

$$\begin{aligned}\dot{w} &= A(0)\left(W_{20}(\theta)\frac{z^2}{2} + W_{11}(\theta)z\bar{z} + W_{02}(\theta)\frac{\bar{z}^2}{2} + \cdots\right)\\ &\quad + H_{20}(\theta)\frac{z^2}{2} + H_{11}(\theta)z\bar{z} + H_{02}(\theta)\frac{\bar{z}^2}{2} + \cdots\\ &= (A(0)W_{20}(\theta) + H_{20}(\theta))\frac{z^2}{2} + (A(0)W_{11}(\theta) + H_{11}(\theta))z\bar{z}\\ &\quad + (A(0)W_{02}(\theta) + H_{02}(\theta))\frac{\bar{z}^2}{2} + \cdots .\end{aligned} \tag{3.28}$$

Comparing the coefficients of z^2 and $z\bar{z}$ from (3.27) and (3.28), we get

$$\begin{aligned}(A(0) - 2i\omega^*\tau^*I)W_{20}(\theta) &= -H_{20}(\theta),\\ A(0)W_{11}(\theta) &= -H_{11}(\theta).\end{aligned} \tag{3.29}$$

For $\theta \in [0, 1]$, it follows from (3.16), (3.17), (3.26) and (3.27) that

$$\begin{aligned}H(z,\bar{z},\theta) &= -\bar{q}^*(0)f_0q(\theta) - q^*(0)\bar{f}_0\bar{q}(\theta) = -g(z,\bar{z})q(\theta) - \bar{g}(z,\bar{z})\bar{q}(\theta),\\ &= -\left(g_{20}\frac{z^2}{2} + g_{11}z\bar{z} + g_{02}\frac{\bar{z}^2}{2} + \cdots\right)q(\theta)\\ &\quad -\left(\bar{g}_{20}\frac{\bar{z}^2}{2} + \bar{g}_{11}z\bar{z} + \bar{g}_{02}\frac{z^2}{2} + \cdots\right)\bar{q}(\theta).\end{aligned} \tag{3.30}$$

Comparing the coefficients of z^2 and $z\bar{z}$ between (3.26) and (3.30), we get

$$\begin{aligned}H_{20}(\theta) &= -g_{20}q(\theta) - \bar{g}_{02}\bar{q}(\theta),\\ H_{11}(\theta) &= -g_{11}q(\theta) - \bar{g}_{11}\bar{q}(\theta).\end{aligned} \tag{3.31}$$

It follows from (3.31), (3.29) and the definition of $A(\theta)$ that

$$\dot{W}_{20}(\theta) = 2i\omega^*\tau^*W_{20}(\theta) + g_{20}q(\theta) + \bar{g}_{02}\bar{q}(\theta), \tag{3.32}$$

$$\dot{W}_{11}(\theta) = g_{11}q(\theta) + \bar{g}_{11}\bar{q}(\theta). \tag{3.33}$$

Since $q(\theta) = (q_1, q_2)^T e^{i\omega^*\tau^*\theta}$, we obtain

$$W_{20}(\theta) = \frac{ig_{20}}{\omega^*\tau^*}q(0)e^{i\omega^*\tau^*\theta} + \frac{i\bar{g}_{02}}{3\omega^*\tau^*}\bar{q}(0)e^{-i\omega^*\tau^*\theta} + E_1 e^{2i\omega^*\tau^*\theta}, \tag{3.34}$$

$$W_{11}(\theta) = \frac{-ig_{11}}{\omega^*\tau^*}q(0)e^{i\omega^*\tau^*\theta} + \frac{i\bar{g}_{11}}{\omega^*\tau^*}\bar{q}(0)e^{-i\omega^*\tau^*\theta} + E_2, \tag{3.35}$$

where $E_1 = (E_1^{(1)}, E_1^{(2)})^T$ and $E_2 = (E_2^{(1)}, E_2^{(2)})^T$ are constant vectors. Now, we focus on the computation of E_1 and E_2. From the definition of $A(0)$ and (3.33), we have

$$\int_{-1}^{0} d\eta(\theta)W_{20}(\theta) = 2i\omega^*\tau^*W_{20}(0) - H_{20}(0), \tag{3.36}$$

and

$$\int_{-1}^{0} d\eta(\theta)W_{11}(\theta) = -H_{11}(0), \tag{3.37}$$

where $\eta(\theta) = \eta(\theta, 0)$. In view of (3.25), we induce that when $\theta = 0$,

$$\begin{aligned} H(z, \bar{z}, 0) &= -2Re\{\bar{q}^*(0)f_0q(0)\} + f_0 \\ &= -g(z, \bar{z})q(0) - \bar{g}(z, \bar{z})\bar{q}(0) + f_0. \end{aligned} \tag{3.38}$$

Then we have

$$\begin{aligned} H_{20}\frac{z^2}{2} + H_{11}z\bar{z} + H_{02}\frac{\bar{z}^2}{2} + \cdots = &-\left(g_{20}\frac{z^2}{2} + g_{11}z\bar{z} + g_{02}\frac{\bar{z}^2}{2} + \cdots\right)q(0) \\ &-\left(\bar{g}_{20}\frac{\bar{z}^2}{2} + \bar{g}_{11}z\bar{z} + \bar{g}_{02}\frac{z^2}{2} + \cdots\right)\bar{q}(0) + f_0. \end{aligned} \tag{3.39}$$

Comparing both sides of (3.39), we obtain

$$H_{20} = -g_{20}q(0) - \bar{g}_{02}\bar{q}(0) + 2\tau^*(H_1, H_2)^T, \tag{3.40}$$

$$H_{11} = -g_{11}q(0) - \bar{g}_{11}\bar{q}(0) + \tau^*(P_1, P_2)^T, \tag{3.41}$$

where $H \triangleq (H_1, H_2)^T$ and $P \triangleq (P_1, P_2)^T$ are respectively the coefficients of z^2 and $z\bar{z}$ of $f_0(z, \bar{z})$. Thus we have

$$H = \begin{pmatrix} -cq_2e^{-i\omega^*\tau^*} - \frac{rK^2(1+a)}{(K+au_1^*)^3} \\ 0 \end{pmatrix}, \tag{3.42}$$

and

$$P = 2\begin{pmatrix} -\frac{rK^2(1+a)}{(K+au_1^*)^3} - cRe\{\bar{q}_2 e^{i\omega^*\tau^*}\} \\ 0 \end{pmatrix}. \tag{3.43}$$

Since $i\omega^*\tau^*$ is the eigenvalue of $A(0)$ and $q(0)$ is the corresponding eigenvector, we get

$$\left(i\omega^*\tau^* I - \int_{-1}^{0} e^{i\omega^*\tau^*\theta} d\eta(\theta)\right) q(0) = 0, \tag{3.44}$$

and

$$\left(-i\omega^*\tau^* I - \int_{-1}^{0} e^{-i\omega^*\tau^*\theta} d\eta(\theta)\right) \bar{q}(0) = 0. \tag{3.45}$$

Therefore, substituting (3.36) and (3.44) into (3.45), we have

$$\left(2i\omega^*\tau^* I - \int_{-1}^{0} e^{2i\omega^*\tau^*\theta} d\eta(\theta)\right) E_1 = 2\tau^* H, \tag{3.46}$$

that is

$$H^* E_1 = 2H, \tag{3.47}$$

where

$$H^* = \begin{pmatrix} 2i\omega^* + k^\gamma D_1 + \frac{rK^2(1+a)}{(K+au_1^*)^2} & cu_1^* e^{-2i\omega^*\tau^*} \\ -be^{-2iw^*\tau^*} & 2i\omega^* + k^\gamma D_2 + d \end{pmatrix}. \tag{3.48}$$

It follows that

$$E_1 = \frac{2}{\triangle}\begin{pmatrix} (2i\omega^* + k^\gamma D_2 + d)(-cq_2 e^{-i\omega^*\tau^*} - \frac{rK^2(1+a)}{(K+au_1^*)^3}) \\ be^{-2i\omega^*\tau^*}(-cq_2 e^{-i\omega^*\tau^*} - \frac{rK^2(1+a)}{(K+au_1^*)^3}) \end{pmatrix}, \tag{3.49}$$

where $\triangle = Det(H^*)$. In a similar way, we can get

$$P^* E_2 = 2P, \tag{3.50}$$

where

$$P^* = \begin{pmatrix} k^\gamma D_1 + \frac{rK^2(1+a)}{(K+au_1^*)^3} & cu_1^* \\ -b & k^\gamma D_2 + d \end{pmatrix}. \tag{3.51}$$

It follows that

$$E_2 = \frac{2}{\tilde{\Delta}} \begin{pmatrix} (k^\gamma D_2 + d)(\frac{-rk^2(1+a)}{(K+au_1^*)^3} - cRe\{\bar{q}_2 e^{i\omega^*\tau^*}\}) \\ b(\frac{-rk^2(1+a)}{(K+au_1^*)^3} - cRe\{\bar{q}_2 e^{i\omega^*\tau^*}\}) \end{pmatrix}, \tag{3.52}$$

where $\tilde{\Delta} = Det(P^*)$. Thus, we can determine $W_{20}(\theta)$ and $W_{11}(\theta)$ from (3.34) and (3.35). Furthermore, g_{21} can be expressed explicity.

By [21], the Hopf bifurcation periodic solutions of the system (1.1) at τ^* on the center manifold are determined by the following formulas

$$\begin{aligned} C_1(0) &= \frac{i}{2\tau^*\omega^*}\left(g_{11}g_{20} - 2|g_{11}|^2 - \frac{|g_{02}|^2}{3}\right) + \frac{g_{21}}{2}, \\ \nu_2 &= -\frac{Re\{C_1(0)\}}{Re\{\frac{d\lambda}{d\tau}(\tau^*)\}}, \\ \beta_2 &= 2Re\{C_1(0)\}, \\ T_2 &= \frac{-Im\{C_1(0)\} + \nu_2 Im\{\frac{d\lambda}{d\tau}(\tau^*)\}}{\tau^*\omega^*}. \end{aligned} \tag{3.53}$$

Here ν_2 determines the direction of Hopf bifurcation. If $\nu_2 > 0$ ($\nu_2 < 0$), then the Hopf-bifurcation is forward (backword). β_2 determines the stability of the bifurcating periodic solutions. If $\beta_2 < 0$ ($\beta_2 > 0$), then the bifurcating periodic solutions are stable (unstable). T_2 determines the periods of bifurcation periodic solutions. If $T_2 > 0$ ($T_2 < 0$), then the period increases (decreases). Therefore, we have the following results.

Theorem 3.1 *The Hopf bifurcation of the system* (1.1) *occurring at* $\mathbf{u}^*$ *when* $\tau = \tau^*$ *is forward (backward) if* $\nu_2 > 0$ ($\nu_2 < 0$) *and the bifurcating periodic solutions on the center manifold are stable (unstable) if* $Re\{C_1(0)\} < 0$ (> 0).

4 Numerical results

For numerical study of pattern formation in the system (1.1), we only need consider the dynamics of the perturbation to the homogeneous steady state. Hence we use the periodic boundary conditions and the small-amplitude random initial data to the system (1.1). We can use the pseudospectral method [22] to perform numerical computations with time integration in Fourier space. Moreover, we use a Crank–Nicolson scheme for the linear operator and an Adams–Bashforth scheme for the nonlinear operator [23]. Now we carry out numerical simulation to demonstrate the analytical results. To this end, the domain of system (1.1) is confined to a square domain $\Omega = [0, L] \times [0, L] \subset \mathbb{R}^2$ with $L = 200$.

For numerical simulations, we take the following parameter values

$$r = 1.1, K = 1.1, a = 0.1, b = 0.9, c = 0.8, d = 0.1,$$
$$D_1 = 0.1, D_2 = 0.2, \gamma = 1.5, \tau = 1.55. \tag{4.1}$$

It is easy to check that condition (G_1) are fulfilled. Moreover, this set of parameters gives a unique positive equilibrium

$$(u_1^*, u_2^*) = (0.1327, 1.1947), \tag{4.2}$$

which is locally stable when $\tau < \tau^*$ and unstable when $\tau > \tau^*$, according to Theorem 2.1. Here the critical value τ^* is the smallest value among all τ_k^j, that is, $\tau^* = \tau_k^0 = 1.4168$.

To check the stability and direction of the Hopf bifurcations, we compute the first Lyapunov number $C_1(0)$. Here we only consider the first bifurcation threshold, that is, τ^*. Direction calculation shows that $C_1(0) = -0.5153 - 5.0739i$, that is, $Re\{C_1(0)\} < 0$, which means that the bifurcating periodic solution from the spatially uniform equilibrium is asymptotically stable.

It is well-known that for a purely spatial homogeneous initial distribution, the system always sustains homogeneous and the spatial pattern does not generate. So we take the initial conditions with an inhomogeneous spatial perturbation. Our simulations indicate that the spiral pattern emerges. Moreover, the number of the spiral pattern depends on the number of the defect-point of the initial data. We recall that the defect-point (x_c, y_c) of the initial data means that (x_c, y_c) satisfied that $u_1(x_c, y_c)|_{t=0} = u_1^*$ and $u_2(x_c, y_c)|_{t=0} = u_2^*$.

Here we present the results of two computer experiments differing in the form of the initial conditions.

In the first case, the initial distribution of species is given in the following form:

$$u_1(x, y, t) = u_1^* + \epsilon_1(x - 100)$$
$$u_2(x, y, t) = u_2^* - \epsilon_2(y - 100),$$

where $\epsilon_1 = 5 \times 10^{-4}$, $\epsilon_2 = 3 \times 10^{-3}$. In this case the initial data contains only one defect-point $(x_c, y_c) = (100, 100)$. Snapshots of u_1 are shown in Fig. 1 (spatial patterns of u_2 are qualitatively similar except for the early stages of the process when the influence of the initial condition dominates). One spiral emerges around the defect-point (Fig. 1a). The spiral grows gradually in (Fig. 1b, c). Eventually, the regular spatial spiral prevails over the whole domain (Fig. 1d).

In the second case, the initial distribution of species is given in the following form:

$$u_1(x, y, t) = u_1^* + \epsilon_3(x - 80)(x - 140) + \epsilon_4(y - 60)(y - 140),$$
$$u_2(x, y, t) = u_2^* - \epsilon_5(x - 100) - \epsilon_6(y - 180),$$

where $\epsilon_3 = 1 \times 10^{-5}$, $\epsilon_4 = 4 \times 10^{-5}$, $\epsilon_5 = 2 \times 10^{-2}$ and $\epsilon_6 = 1 \times 10^{-3}$. In this case, the initial data contains two defect-points $(x_c, y_c) = (106.1767, 56.4669)$ and $(x_c, y_c) = (104.0321, 143.3332)$. The pattern formation processes are shown in Fig. 2. Two spiral simultaneously emerges around the defect-point (Fig. 2a). The

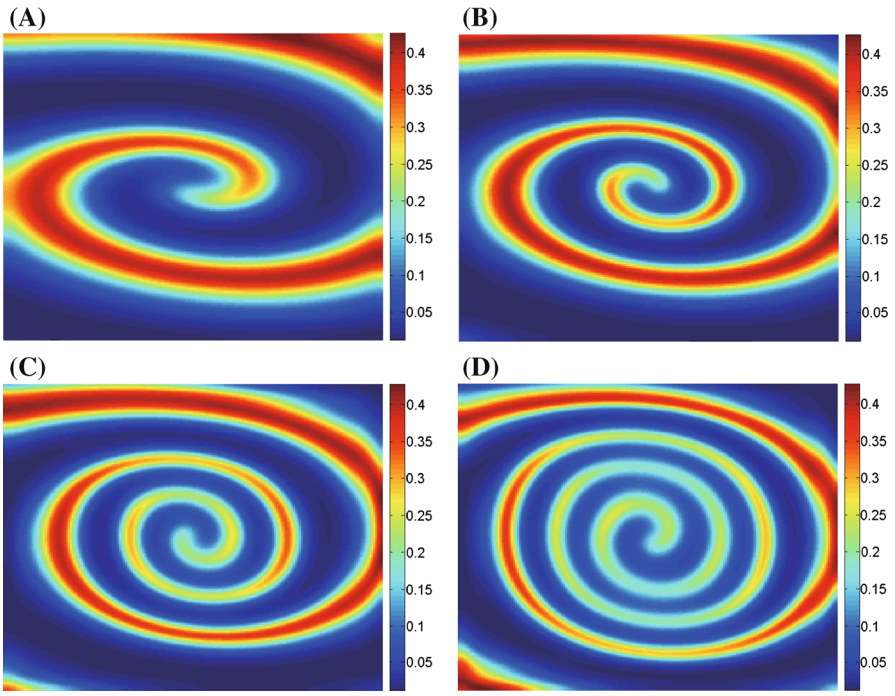

Fig. 1 *Snapshots* of one *spiral* wave at different time. **a** $t = 200$, **b** $t = 400$, **c** $t = 600$, **d** $t = 800$

spirals grow gradually in (Fig. 2b, c). Eventually, the two spatial spirals prevail over the whole domain (Fig. 2d).

5 Discussion

In this paper, we have developed a theoretical framework for studying the phenomenon of pattern formation in a fractional reaction-diffusion system with time delays. It was found (Theorems 2.1 and 2.2) that, apart from the anomalous diffusion-driven Turing patterns, spatial spiral patterns can also arise as a consequence of Hopf bifurcation when the bifurcation parameter, i.e., time delay τ goes beyond a threshold value τ^*. Moreover, we attempted to answer why the emerging spatial spiral patterns are sensitive to initial data. Theorem 3.1 shows that the robustness is due to the existence of stable bifurcating periodic solutions, which leads to spatially inhomogeneous distribution of species density.

Lévy flights are stochastic process characterised by the occurrence of extremely long jumps such that the same sites are revisited much less frequently than in a normal diffusion process. The length of these jumps is distributed according to Lévy stable statistics with a power law tail and divergence of the second moment, which strongly contradicts the ordinary Brownian motion for which all moments of the particle coordinate are finite. The power law tail is also termed as "fat-tailed distribution" because the tail falls off much more gently than for a Gaussian distribution. It is the property

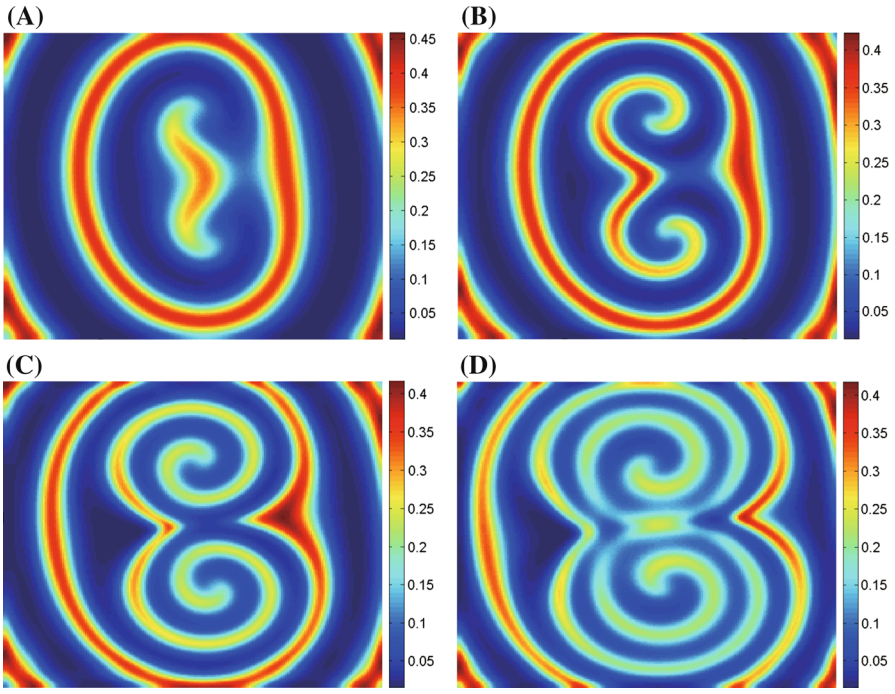

Fig. 2 *Snapshots* of two *spirals* wave at different time. **a** $t = 200$, **b** $t = 400$, **c** $t = 600$, **d** $t = 800$

that lies at the heart of the interesting and unusual behaviour of Lévy flights. Realisation of the Lévy flights in physical phenomena are very diverse such as in fluid dynamics, dynamical systems, and micelles [24]. Recent field study in ecology provided convincing evidence for the existence of Lévy flights among the foraging of marine predators ranging across natural landscapes [25,26]. It was found that Lévy flights are expected in places where prey is scare (e.g., less productive waters such as the open ocean) while Brownian strategy is more likely to occur where prey is abundant (e.g., the productive shelf or convergence-front habitats). These two foraging strategies can be alternately performed by some individuals and which is the ongoing strategy depends on the gradients of environment that the individuals are involved in. Our feedback model can help to clarify spiral patterns of species interactions with Lévy distribution. The proposed approach has applicability to other reaction-diffusion systems including delays, such as competition model and mutualistic model.

References

1. Y.L. Song, S.L. Yuan, Bifurcation analysis for a regulated logistic growth model. Appl. Math. Model. **31**, 1729–1738 (2007)
2. Z. Li, M. Han, F. Chen, Influence of feedback controls on an autonomous Lotka–Volterra competitive system with infinite delays. Nonlinear Anal. RWA **14**, 402–413 (2013)
3. I. Turner, M. Ilić, P. Perr, The use of fractional-in-space diffusion equations for describing microscale diffusion in porous media, in: *11th International drying conference*, (Magdeburg, Germany, 2010)

4. S. Whitaker, Flow in porous media I: A theoretical derivation of Darcy's law. Transp. Porous Media **1**, 3–25 (1986)
5. R. Metzler, J. Klafter, The random walk's guide to anomalous diffusion: A fractional dynamics approach. Phys. Rep. **339**, 1–77 (2000)
6. P. Becker-Kern, M.M. Meerschaert, H.P. Scheffler, Limit theorem for continuous time random walks with two time scales. J. Appl. Probab. **41**, 455–466 (2004)
7. Y. Zhang, D.A. Benson, D.M. Reeves, Time and space nonlocalities underlying fractional-derivative models: Distinction and literature review of field applications. Adv. Water Res. **32**, 561–581 (2009)
8. U. Hornung, *Homogenization and Porous Media* (Springer, New York, 1997)
9. M.M. Meerschaert, J. Mortensenb, S.W. Wheatcraft, Fractional vector calculus for fractional advection-dispersion. Phys. A **367**, 181–190 (2006)
10. M. Riesz, Lintegrale de Riemann–Liouville et le probleme de Cauchy. Acta Math. **81**, 1–222 (1949)
11. J.P. Bouchaud, A. Georges, Anomalous diffusion in disordered media: Statistical mechanisms, models and physical applications. Phy. Rep. **195**, 127–293 (1990)
12. V.V. Gafiychuk, B.Y. Datsko, Pattern formation in a fractional reaction-diffusion system. Phys. A **365**, 300–306 (2006)
13. B.I. Henry, T.A.M. Langlands, S.L. Wearne, Turing pattern formation in fractional activator-inhibitor systems. Phys. Rev. E **72**, 026101 (2005)
14. M. Weiss, H. Hashimoto, T. Nilsson, Anomalous protein diffusion in living cells as seen by fluorescence correlation spectroscopy. Biophys. J. **84**, 4043–4052 (2003)
15. A.A. Golovin, B.J. Matkowsky, V.A. Volpert, Turing pattern formation in the Brusselator model with superdiffusion. SIAM J. Appl. Math. **69**, 251–272 (2008)
16. G. Gambino, M.C. Lombardo, M. Sammartino, Turing pattern formation in the Brusselator system with nonlinear diffusion. Phys. Rev. E **88**, 042925 (2013)
17. L. Zhang, C. Tian, Turing pattern dynamics in an activator-inhibitor system with superdiffusion. Phys. Rev. E **90**, 062915 (2014)
18. Y. Nec, A.A. Nepomnyashchy, A.A. Golovin, Oscillatory instability in super-diffusive reaction-diffusion systems: Fractional amplitude and phase diffusion equations. Europhys. Lett. **82**, 58003 (2008)
19. H.I. Freedman, V.S.H. Rao, The trade-off between mutual interference and time lags in predator-prey system. Bull. Math. Biol. **45**, 991–1004 (1983)
20. S.G. Ruan, J.J. Wei, On the zero of some transcendental functions with applications to stability of delay differential equations with two delays. Dyn. Contin. Discrete impuls. Sys. Ser. A Math. Anal. **10**, 863–874 (2003)
21. B. Hassard, D. kazarino, Y. Wan, *Theory and Applications of Hopf Bifurcation* (Cambridge University Press, Cambridge, 1981)
22. W. Huang, D.M. Sloan, A simple adaptive grid method in two dimensions. SIAM J. Sci. Comput. **15**, 776–797 (1994)
23. Y. He, W. Sun, Stability and convergence of the Crank–Nicolson/Adams–Bashforth scheme for the time-dependent Navier–Stokes equations. SIAM J. Numer. Anal. **45**, 837–869 (2007)
24. M.G. Shlesinger, G.M. Zaslavsky, U. Frisch, *Lévy Flights and Related Topics in Physics* (Springer, Berlin, 1995)
25. N.E. Humphries, N. Queiroz, J.R.M. Dyer et al., Environmental context explains Lévy and Brownian movement patterns of marine predators. Nature **465**, 1066 (2010)
26. G.M. Viswanathan, Fish in Lévy-flight foraging. Nature **465**, 1018 (2010)